

# Formation of Light-Absorbing Organosulfates during Evaporation of Secondary Organic Material Extracts in the Presence of Sulfuric Acid

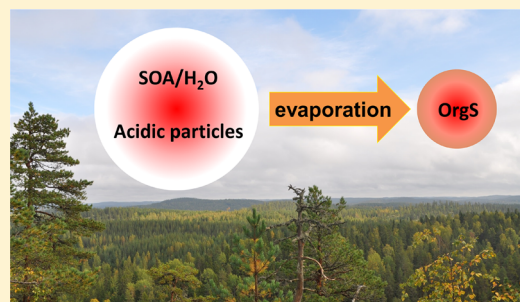
Lauren T. Fleming,<sup>†</sup> Nujhat N. Ali,<sup>†</sup> Sandra L. Blair,<sup>†,§</sup> Marie Roveretto,<sup>‡</sup> Christian George,<sup>‡</sup> and Sergey A. Nizkorodov<sup>\*,†</sup>

<sup>†</sup>Department of Chemistry, University of California, Irvine, Irvine, California 92697, United States

<sup>‡</sup>Univ Lyon, Université Claude Bernard Lyon 1, CNRS, IRCELYON, F-69626 Villeurbanne, France

**ABSTRACT:** Organic aerosols affect the climate by scattering or absorbing incoming solar radiation. Secondary organic material (SOM), which represents the major chemical constituent of atmospheric aerosol particles, is produced by the oxidation of atmospheric volatile organic compounds (VOCs). SOM in clouds, fogs, and aerosols undergoes concentration/dilution cycles due to the evaporation/condensation of water droplets. These physical processes could lead to the chemical processing of SOM and the formation of new, light-absorbing compounds. In this study, model SOM was generated through smog chamber photooxidation and flow tube ozonolysis of various atmospherically relevant anthropogenic and biogenic VOCs, including toluene (TOL), D-limonene (LIM),  $\alpha$ -pinene (APIN),  $\beta$ -pinene (BPIN), and isoprene (ISO). Collected SOM was extracted in water, and the solutions were acidified with sulfuric acid to pH 2 and dried to simulate the evaporation of acidic particles containing SOM. Significant changes in mass absorption coefficients (MACs) were observed after the evaporation and redissolution of SOM in the presence of sulfuric acid. At visible wavelengths, the MAC values of most SOM increased after the evaporation, with the fractional increase being the largest for LIM/O<sub>3</sub> SOM at 400 nm (fractional increase of 65.0). Exceptions to evaporation increasing MAC values in the presence of sulfuric acid were ISO/OH and TOL/OH/NO<sub>x</sub>. Light-absorbing species in LIM/O<sub>3</sub> SOM were chromatographically separated and detected using a photodiode array detector and a high-resolution electrospray ionization mass spectrometer. The increase in MAC was accompanied by the appearance of more than 300 organosulfate peaks. Five potential brown carbon (BrC) chromophores in LIM/O<sub>3</sub> SOM were separated and assigned chemical formulas, including C<sub>10</sub>H<sub>16</sub>SO<sub>6</sub>, C<sub>10</sub>H<sub>14</sub>SO<sub>6</sub>, C<sub>10</sub>H<sub>16</sub>SO<sub>5</sub>, C<sub>11</sub>H<sub>16</sub>SO<sub>7</sub>, and C<sub>11</sub>H<sub>18</sub>SO<sub>8</sub>. This study suggests that evaporation-driven processes may occur in the atmosphere, substantially modifying the molecular composition and optical properties of SOM. The evaporation of filter extracts from the field or laboratory could similarly produce organosulfates as artifacts if the extract is sufficiently acidic before the evaporation. We recommend that complete drying of particulate matter filter extracts should be avoided in future work.

**KEYWORDS:** brown carbon, mass absorption coefficient, mass spectrometry, cloud processing, filter artifacts, molecular composition



## INTRODUCTION

Observations show that most atmospheric particles are dominated by secondary organic material (SOM) formed by the oxidation of volatile organic compounds (VOCs) by ozone (O<sub>3</sub>), hydroxyl radicals (OH), and other oxidants. Atmospheric VOCs are highly variable, with over 3000 types thought to exist.<sup>1</sup> Trees are a major biogenic source of fragrant VOC molecules, such as D-limonene and  $\alpha$ -pinene.<sup>2</sup> In urban areas, the major sources of VOCs are fossil-fuel combustion and industrial emissions.<sup>3</sup> Aerosols produced from these VOCs directly affect the atmospheric energy balance by absorbing or scattering sunlight, depending on their optical properties. Additionally, aerosols serve as cloud condensation nuclei upon which liquid droplets can form.<sup>4</sup> Aerosols that strongly absorb visible radiation are of particular interest because they may contribute to the warming of the lower atmosphere by absorbing sunlight.<sup>5</sup>

SOM is expected to undergo chemical changes resulting from interactions of particles with sunlight, water, and other atmospheric components. It is important to understand the nature of these changes to better predict the health and climate impacts of atmospheric aerosols. For example, condensed atmospheric water, associated with aerosols, clouds, or fogs, is known to undergo various evaporation/condensation cycles that can induce specific chemical transformations of SOM that need to be understood. These processes can be accompanied by the formation of new compounds, such as esters of sulfuric acid known as organosulfates, with the help of acid catalysis by

Special Issue: New Advances in Organic Aerosol Chemistry

Received: February 14, 2019

Revised: May 15, 2019

Accepted: May 16, 2019

Published: May 16, 2019

**Table 1. Names and Abbreviations of VOCs Used To Generate SOM Samples from OH Photooxidation in the Smog Chamber<sup>a</sup>**

precursor	oxidant	initial VOC (ppm)	initial NO (ppb)	reaction time (h)	collection time (h)	typical amount collected (mg)
D-limonene (LIM)	OH	1	0	2	2.5	2.0
D-limonene (LIM)	OH/NO <sub>x</sub>	1	500	2	3	2.9
α-pinene (APIN)	OH	1	0	3	2.5	1.6
α-pinene (APIN)	OH/NO <sub>x</sub>	1	500	2.5	2.5	2.2
isoprene (ISO)	OH	15	0	5.5	3	0.3
isoprene (ISO)	OH/NO <sub>x</sub>	15	500	4	2.5	2.7
toluene (TOL)	OH	1	0	3.5	3	0.9
toluene (TOL)	OH/NO <sub>x</sub>	1	500	3	2	1.6

<sup>a</sup>SOM samples are hereafter referred to as VOC/OH, if prepared under low-NO<sub>x</sub> conditions, and VOC/OH/NO<sub>x</sub>, if prepared under high-NO<sub>x</sub> conditions. The reaction time in the chamber is equivalent to the irradiation time, and no seed aerosol was used in these experiments.

sulfuric acid, which is commonly found in fog droplets and aerosol particles.<sup>6</sup> The mechanisms by which organosulfates are formed could be through alcohol esterification<sup>7–9</sup> and the ring opening of epoxides by sulfuric acid,<sup>8–10</sup> both of which are acid-catalyzed. Under ambient conditions, it is kinetically unlikely that the former mechanism is responsible for organosulfate formation; however, not many studies have examined organosulfate formation in evaporating droplets, which can have much lower pH and higher concentrations of SOM. The acid-catalyzed ring opening of epoxides by sulfate is kinetically favored under ambient conditions,<sup>8–10</sup> and represents a more common mechanism of organosulfate formation. For example, Budisulistiorini and coworkers found that isoprene epoxidol (IEPOX) SOA from field measurements was correlated with observations of organosulfates using positive matrix factorization analysis.<sup>11</sup>

The evaporation of cloud and fog droplets containing SOM and sulfuric acid not only produces new compounds but also can make SOM light-absorbing. A previous study by Nguyen et al.<sup>12</sup> found that light-absorbing chromophores were produced when aqueous extracts of SOM generated from D-limonene ozonolysis, acidified to pH 2 with sulfuric acid, were evaporated. The evaporation of acidified D-limonene SOM extracts was found to significantly accelerate otherwise slow aqueous-phase acid-catalyzed aldol condensation reactions and lead to the formation of sulfur-containing organic compounds. Simultaneously, substantial changes in the optical properties of the SOM extract were observed.

The effects of evaporation in the presence of sulfuric acid on the optical properties of SOM other than D-limonene SOM have not been studied. This study focused on the evaporative browning of model biogenic and anthropogenic SOM in the presence or absence of sulfuric acid. In addition, we explored the effect of the extraction solvent and the amount of solution on the mass absorption coefficient of the material produced during the evaporation. The goals of this work were two-fold: first, to obtain a better understanding of the optical properties and, second, to characterize chromophores and major products of SOM undergoing evaporative browning. The evaporation of SOM extracts in the presence of sulfuric acid enhanced the absorbance of visible wavelengths for most precursor/oxidant combinations and produced organosulfates.

## MATERIALS AND METHODS

**SOM Generation.** Model SOM was prepared from VOCs using O<sub>3</sub>-initiated oxidation and OH-initiated photooxidation conditions, with and without added NO<sub>x</sub>, as shown in Tables 1 and 2. VOCs, including isoprene (ISO), α-pinene (APIN), β-

**Table 2. Names and Abbreviations of VOCs Used To Generate SOM Samples from Flow Tube Ozonolysis<sup>a</sup>**

precursor	initial VOC (ppm)	typical amount collected (mg)
D-limonene (LIM)	10	4.0
α-pinene (APIN)	10	2.4
β-pinene (BPIN)	10	2.0

<sup>a</sup>Initial VOC concentration in flow tube experiments is the steady-state mixing ratio the VOC would have in the absence of ozone. Ozone was added in small excess with respect to the VOC. The flow tube residence time is on the order of minutes. The SOM samples are hereafter referred to as VOC/O<sub>3</sub>.

pinene (BPIN), D-limonene (LIM), and toluene (TOL), were used as purchased from Sigma-Aldrich (typically >99% pure) without further purification.

SOM generation by photooxidation occurred in a ~5 m<sup>3</sup> Teflon chamber, equipped with UV-B lights (FS40T12/UVB, Solarc Systems) with emission centered at 310 nm. The reactions took place under dry conditions (relative humidity <2%) in the absence of seed particles. Chamber experiments were carried out either under “high-NO<sub>x</sub>” oxidation conditions, with ~500 ppb (parts per billion by volume) of NO added to the chamber to simulate an urban atmospheric environment, or “low-NO<sub>x</sub>” oxidation conditions, without any NO added to the chamber to simulate a remote atmospheric environment. For the OH precursor, 90 μL of H<sub>2</sub>O<sub>2</sub> (Sigma-Aldrich; 30% by volume; certified ACS grade) was injected into the chamber by evaporation under a stream of zero air, resulting in 5 ppm of H<sub>2</sub>O<sub>2</sub> vapor in the chamber. Precursor VOC was added to the chamber using the same method, with the starting VOC mixing ratio in the chamber on the order of 1 ppm. The starting mixing ratio of isoprene, however, was larger at 15 ppm, and H<sub>2</sub>O<sub>2</sub> was increased to 10 ppm to generate adequate SOM mass loadings for the evaporation experiments. The chamber contents were mixed for several minutes using a fan, which was then turned off to minimize particle wall losses. The UV-B lamps were turned on for 2–5.5 h to initiate photochemistry (Table 1). SOM particle concentration within the chamber was monitored by a TSI model 3936 scanning mobility particle sizer (SMPS). A Thermo Scientific model 49i ozone analyzer recorded O<sub>3</sub> data, while a Thermo Scientific model 42i-Y NO<sub>y</sub> analyzer recorded NO/NO<sub>y</sub> data. SOM passed through an activated carbon denuder at ~18 SLM (standard liters per minute) and particles were collected using PTFE filters (0.2 μm pore size, 47 mm diameter, Millipore Fluoropore). Collection times ranged from 2 to 3 h, with approximately 0.3 to 2.9 mg of SOM collected on the filter, depending on the sample. The amount of SOM on the filter

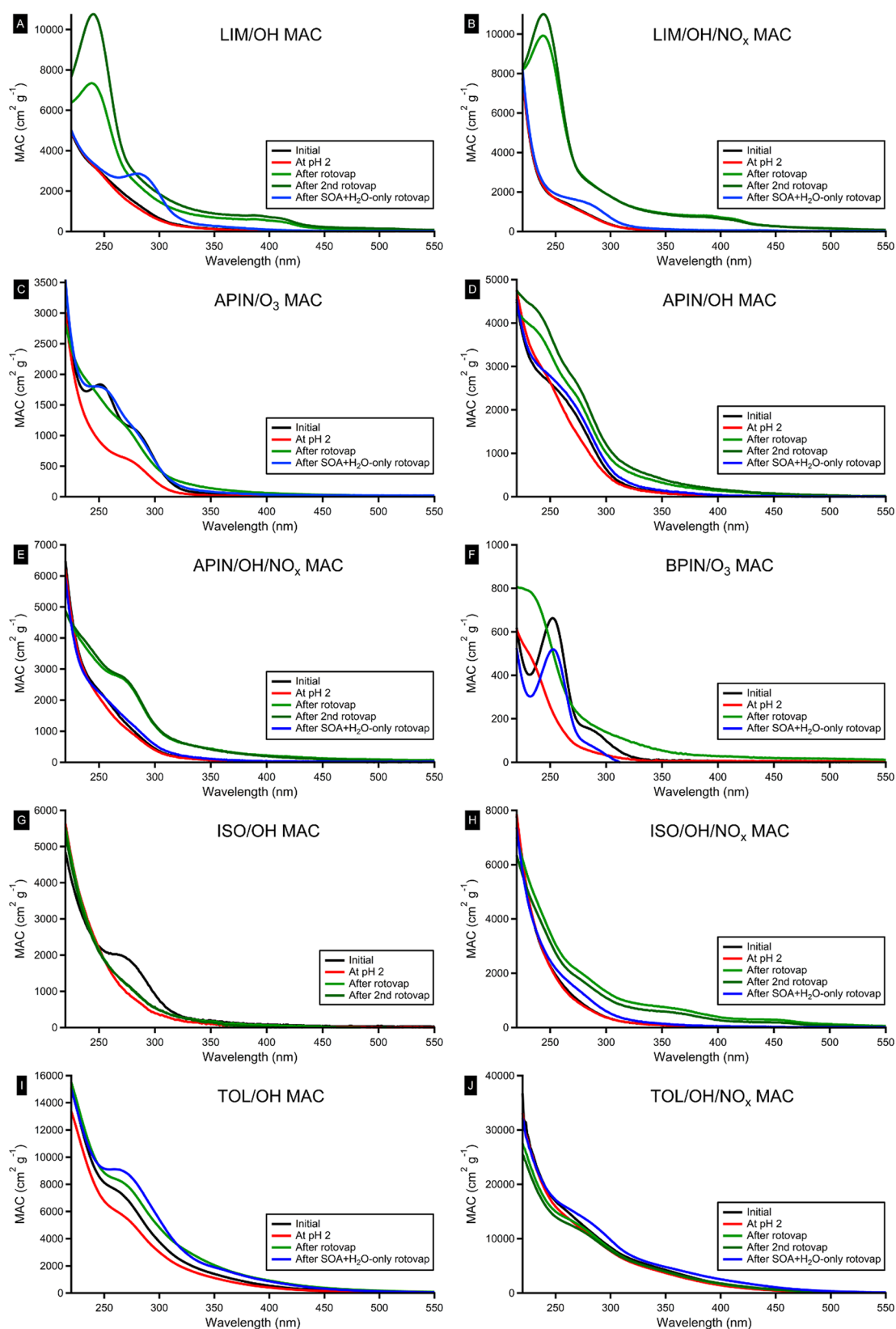


**Figure 1.** MAC values of SOM from (A) LIM/OH, (B) LIM/OH/NO<sub>x</sub>, (C) APIN/O<sub>3</sub>, (D) APIN/OH, (E) APIN/OH/NO<sub>x</sub>, (F) BPIN/O<sub>3</sub>, (G) ISO/OH, (H) ISO/OH/NO<sub>x</sub>, (I) TOL/OH, and (J) TOL/OH/NO<sub>x</sub> in initial aqueous solution (black), after the addition of H<sub>2</sub>SO<sub>4</sub> to the solution until it reached pH 2 (red), after the evaporation of acidified solution (green), after the second evaporation of the same solution (dark green), and after the evaporation with SOM and water only (blue).

was estimated from SMPS data, assuming a particle density of  $1.2 \text{ g/cm}^3$  and 100% collection efficiency by the filters. This

particle density reflects representative average densities of anthropogenic and biogenic SOM reported by Hallquist et al.<sup>13</sup>

In several cases, the amount was verified by explicit weighing of the filter. The SMPS and filter-based measurements of the collected SOM mass were typically within 35% of each other. This discrepancy could be due to the evaporation of semivolatile compounds from filters under ambient conditions, inaccurately assuming SOM density that is an important factor for calculating mass concentrations on SMPS, or wall losses during SOM collection, which could result in the over-prediction of filter mass.

The O<sub>3</sub>-initiated reactions were carried out in a 17 L flow tube reactor described by Bones et al.<sup>14</sup> Liquid VOC was injected by a syringe pump at a rate of 25 μL/h into a 5 SLM flow of zero air. A 0.5 SLM flow of oxygen (Airgas; 99.994% purity) was sent through an ozone generator and a custom-made ozone photometric detector. The flows containing VOC and ozone were mixed at the entrance of the flow cell. Typical mixing ratios in the flow cell ranged from 60 to 100 ppm (parts per million by volume) of O<sub>3</sub> and 10 ppm of VOC. The residence time in the flow tube was <5 min, but this was sufficient to oxidize most of the VOC and to form SOM. A 1 m charcoal denuder scrubbed the residual O<sub>3</sub> and gas-phase organic compounds from the aerosol flow exiting the reactor. SOM was collected on preweighed polytetrafluoroethylene (PTFE) filters (Millipore Fluoropore, 0.2 μm pore size). Depending on the yield of SOM, collection time for the flow tube was ~30 min to 2 h. The samples were either immediately analyzed or sealed and frozen for future analysis. The amount of SOM on the filter was determined by weighing. The reaction conditions are summarized in Table 2.

**SOM Extraction.** In most experiments, the SOM was extracted into water by placing the filter on the bottom of a beaker, adding water, and shaking the beaker for about 1 h. The amount of water was adjusted in each sample to obtain stock solutions with the same mass concentrations (~0.3 mg/mL) of the dissolved organics. The extraction was estimated to be at least 90% complete based on the comparison of the absorption spectra of the primary and secondary extracts from the same filter.<sup>15</sup> A fresh solution was prepared for each experiment and used immediately. In a few LIM/O<sub>3</sub> experiments, methanol or acetonitrile was used as an extracting solvent instead of water because all three solvents are commonly used to extract SOM.

**Evaporation Experiments and MAC Measurements.** A 2 mL aliquot of the SOM extract was transferred in a 1 cm quartz cuvette, and a UV/vis absorption spectrum was taken in a dual-beam spectrophotometer (Shimadzu UV-2450), with another cuvette filled with the pure solvent used as reference. For samples that were acidified, the pH of the solution was adjusted to pH 2 using sulfuric acid, such that the volume of the sample solution did not increase by more than 300 μL (<15%), and the UV/vis spectrum was recorded again. The pH of the solution was measured with a Mettler Toledo SevenEasy S20 pH meter.

The solution was then transferred to a 20 mL vial and evaporated to near-dryness using a rotary evaporator (Buchi R-210) at a water bath temperature of 50 °C. The evaporation rate was constant when using a particular solvent, as the water temperature was regulated to 50 °C. After evaporation, water was added to the vial to reach the initial pre-evaporation volume. Control experiments were performed in which the same procedure was followed, except for the acidification step. In several cases, the evaporation and redissolution steps were repeated to see if additional browning could be produced by

one more evaporation step. It should be noted that 50 °C is higher than a typical ambient temperature; however, this temperature was chosen to more rapidly evaporate the solution and therefore better simulate the rapid evaporation of cloud and fog droplets. The chemistry could potentially depend on temperature, but we have not explored this temperature dependence in this study.

Wavelength-dependent mass absorption coefficients (MACs), in units of cm<sup>2</sup> g<sup>-1</sup>, were calculated from the base-10 absorbance, A<sub>10</sub>, of each SOM extract with the solution mass concentration, C<sub>mass</sub> (g cm<sup>-3</sup>), and path length, *b* (cm)

$$\text{MAC}(\lambda) = \frac{A_{10}^{\text{solution}}(\lambda) \times \ln(10)}{b \times C_{\text{mass}}} \quad (1)$$

**Brown Carbon (BrC) Chromophore Analysis.** High-performance liquid chromatography coupled to a photodiode array detector and a high-resolution mass spectrometer, referred to as HPLC-PDA-HRMS, was employed for the analysis of BrC chromophores. The evaporated SOM residue was reconstituted in a 60% water/40% acetonitrile by volume solution. The reconstituted extract was injected (5 μL) into a reverse-phase column (Acquity HSS T3 column 2.1 × 100 mm, 1.8 μm) at a flow rate of 0.3 mL/min with a mobile phase gradient utilizing 0.1% formic acid in water (A) or acetonitrile (B) solvents. A 17 min gradient was applied: Eluent (B) was kept at 1% for 2 min and was increased to 100% in 11 min. This composition was maintained for 2 min before returning to the initial condition for 2 min (1% of eluent B). Separated compounds then passed through the PDA to record absorption spectra over a 200–700 nm range before entering the HRMS (Q-Exactive Hybrid Quadrupole-Orbitrap, Thermo Scientific, USA). Compounds were charged by electrospray ionization using the following settings: a spray potential of 3 kV, Aux gas heater temperature of 250 °C, sheath gas flow rate of 42 au, Aux gas flow rate 25 au, capillary temperature 350 °C, and S-lens RF level 50. Ions were subsequently detected within a range of 50–750 *m/z*, with a mass accuracy of 0.5 to 2.0 ppm and a resolving power of 140 000 at *m/z* 200. Data were collected in both negative and positive ion modes using Thermo Xcalibur software (2.2 SP1.48; Thermo Fisher Scientific). BrC chromophores were initially screened in the same software, and ions corresponding to BrC chromophores were further analyzed using the open-source software toolbox MZmine version 2.26.<sup>16</sup> Formula Calculator v1.1 was used to assign neutral chemical formulas to ions of interest.

## RESULTS AND DISCUSSION

**Optical Properties.** Wavelength-dependent MACs for various SOMs during all stages of the experiment are summarized in Figure 1. The first step of the experiment was adjusting the pH of the solution to pH 2 by adding sulfuric acid. In some cases, the pH adjustment had a minimal effect on the absorbance spectrum of the solution (e.g., LIM samples), but for most other SOMs the spectrum changed presumably due to shifting acid–base equilibria for carboxylic acids and possibly due to acid-catalyzed reactions between SOM compounds.

Next, the acidic SOM solution was evaporated in 1–5 min depending on the solvent, and the solution was reconstituted in the initial volume of solvent. Browning was observed to happen quickly when the solution was evaporated to near dryness. To better quantify the extent of evaporation-driven

**Table 3.** MAC Values ( $\text{cm}^2 \text{g}^{-1}$ ) at 300 and 400 nm for All SOM Types after Rotary Evaporation in the Presence of Sulfuric Acid<sup>a</sup>

SOM (precursor/oxidant)	MAC after rotavap ( $\text{cm}^2 \text{g}^{-1}$ , 300 nm)	fractional increase in MAC after rotavap ( $\text{cm}^2 \text{g}^{-1}$ , 300 nm)	MAC after rotavap ( $\text{cm}^2 \text{g}^{-1}$ , 400 nm)	fractional increase in MAC after rotavap ( $\text{cm}^2 \text{g}^{-1}$ , 400 nm)
limonene/OH	$1.48 \times 10^3$	2.61	537	35.0
limonene/OH/ $\text{NO}_x$	$1.77 \times 10^3$	5.23	714	*
$\alpha$ -pinene/ $\text{O}_3$	$5.03 \times 10^2$	1.94	61.4	5.71
$\alpha$ -pinene/OH	$1.01 \times 10^3$	1.96	138	6.00
$\alpha$ -pinene/OH/ $\text{NO}_x$	$1.18 \times 10^3$	2.96	223	9.67
$\beta$ -pinene/ $\text{O}_3$	$1.39 \times 10^2$	4.36	28.3	4.78
isoprene/OH	$3.99 \times 10^2$	1.00	30.7	0.50
isoprene/OH/ $\text{NO}_x$	$1.33 \times 10^3$	3.60	391	12.8
toluene/OH	$4.83 \times 10^3$	1.60	920	2.27
toluene/OH/ $\text{NO}_x$	$8.06 \times 10^3$	1.04	$1.69 \times 10^3$	1.18
limonene/ $\text{O}_3$	$1.13 \times 10^3$	4.74	499	65.0

<sup>a</sup>Fractional increase in MAC ( $\text{MAC}_{\text{after}}/\text{MAC}_{\text{before}}$ ) from evaporation is also given. \* indicates that before evaporation, the MAC was at noise level, and therefore an increase is not quantifiable.

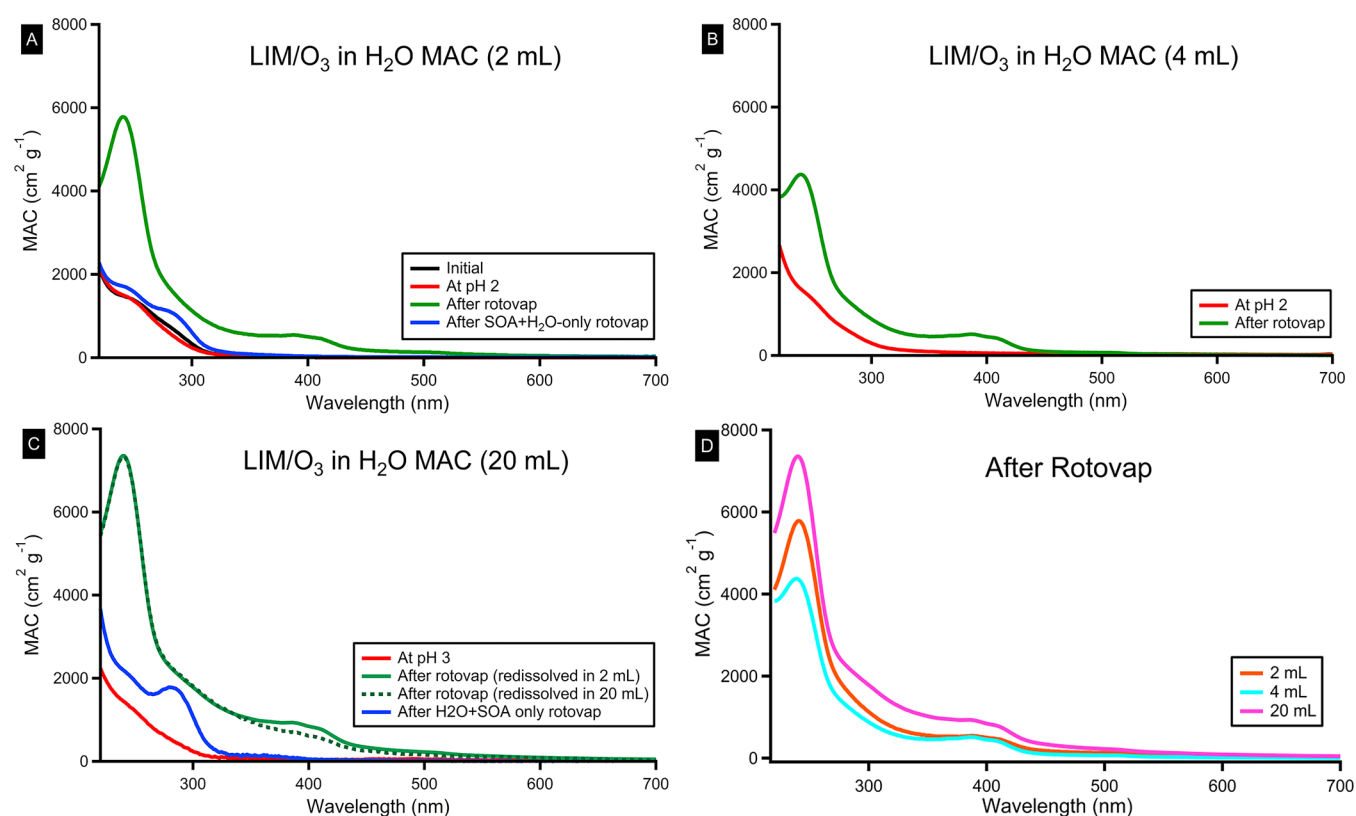


**Figure 2.** MAC values of LIM/ $\text{O}_3$  SOM dissolved in 2 mL of water (black trace in panel A) (black). Also shown are MAC values after the addition of  $\text{H}_2\text{SO}_4$  to pH 2 in 2 mL of water and further dilution to 4 and 20 mL (red), after the evaporation of the solutions (green), and after the evaporation with LIM/ $\text{O}_3$  SOM and water only (blue). (B) The evaporated solution was redissolved in 4 mL of  $\text{H}_2\text{O}$ , and MAC values were calculated (green). (C) The evaporated solution was redissolved first in 2 mL of  $\text{H}_2\text{O}$  (green) and then to a total volume of 20 mL of  $\text{H}_2\text{O}$  (dark dashed green). (D) MAC values for the evaporated solutions from panels A–C are shown on the same graph for comparison.

browning, MAC values at 300 and 400 nm are given in Table 3 for all SOM types, and the percent increase in MAC after the evaporation step is calculated. For most SOMs, evaporation enhanced the MAC values for the visible wavelengths, with the largest fractional increase for the LIM-derived SOM. (400 nm MAC went up by a factor of 35 for LIM/OH and by a factor of 65 for LIM/ $\text{O}_3$ .) Whereas TOL-derived SOM had the highest MAC at 400 nm, it was not strongly affected by the evaporation, resulting in the smallest fractional increase in MAC. (400 nm MAC was essentially unchanged for TOL/OH/ $\text{NO}_x$  and rose by a factor of 2.3 for TOL/OH.) In the

case of TOL/OH/ $\text{NO}_x$ , absorbing nitrophenols are present in SOM to begin with, resulting in the observed large absorbance. Any additional chromophores produced by the evaporation made only a small contribution to the already high absorption coefficients. The BPIN/ $\text{O}_3$  SOM had the lowest observed MAC values after the evaporation. A notable exception to evaporation increasing MAC in the presence of sulfuric acid was ISO/OH SOM, which remained largely unchanged at all wavelengths. It should be noted that ISO/OH SOM was prepared in the absence of acidic sulfate seed particles, which

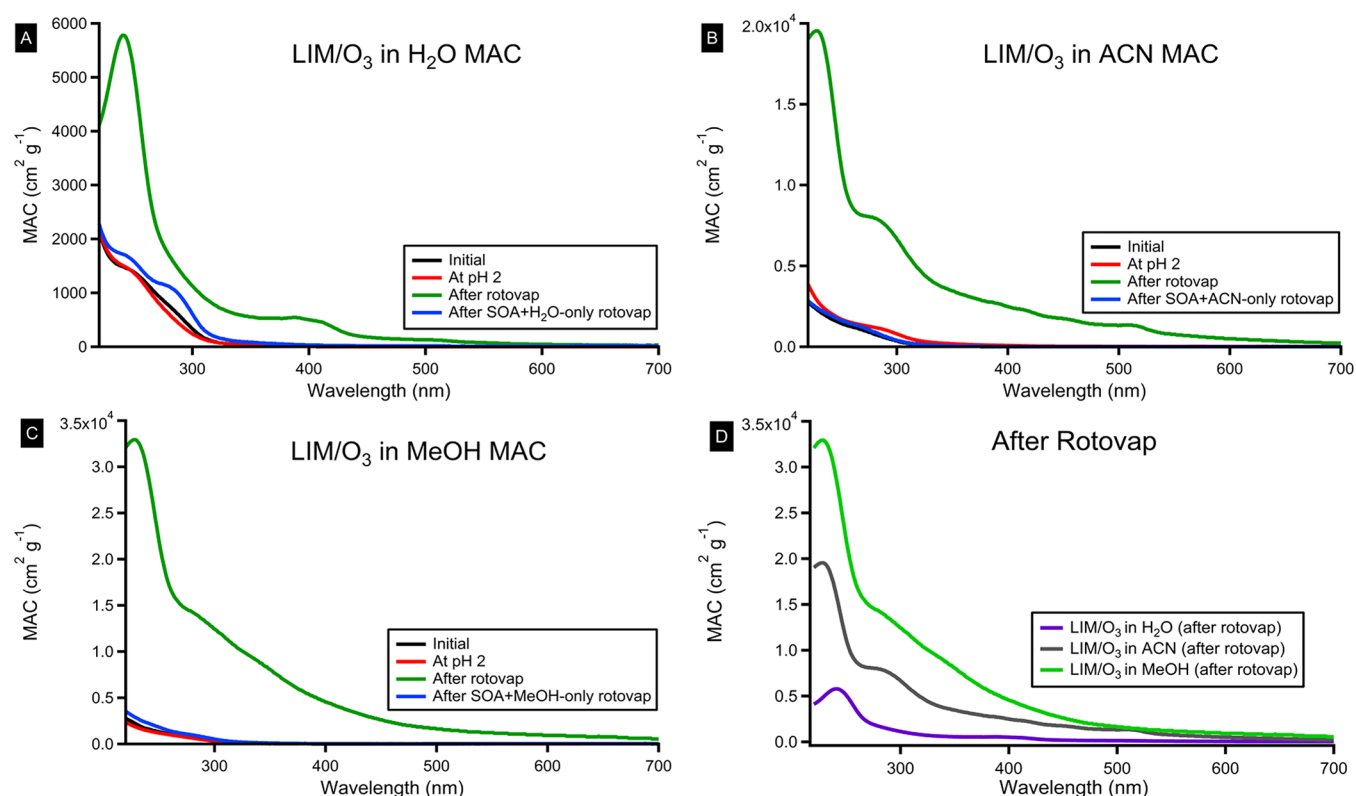


**Figure 3.** MAC values of LIM/O<sub>3</sub> SOM, with the solvent as (A) water, (B) acetonitrile, or (C) methanol, in initial solution (black), after the addition of H<sub>2</sub>SO<sub>4</sub> to pH 2 in water or the addition of an equal amount of H<sub>2</sub>SO<sub>4</sub> in acetonitrile and methanol (red), after the evaporation of solution (green), and after the evaporation with LIM/O<sub>3</sub> SOM and solvent only (blue). (D) MAC values for the evaporated solutions in panels A–C are compared on the same scale.

would likely give a different result from SOM obtained by acid-catalyzed reactive uptake of IEPOX.<sup>17,18</sup>

The effect of evaporating the reconstituted SOM a second time is also shown in Figure 1. The second evaporation produced only minor changes to MAC values compared with the results of the first evaporation. This implies that the evaporative browning proceeded nearly to completion already after the first evaporation step.

Control experiments were performed, where nonacidified SOM solutions were evaporated (blue trace in Figure 1). In most cases, this did not appreciably increase MAC values in the visible wavelength range. However, in the case of TOL/OH, MAC values increased after evaporation by a factor of 2.1 in the absence of sulfuric acid compared with 2.3 in the presence of sulfuric acid. This suggests that different types of BrC chromophores are formed during evaporation for this SOM, which do not require acid catalysis, potentially by oligomerization of hydroxylated aromatic units.

The effect of the starting SOM solution volume is explored for the LIM/O<sub>3</sub> SOM solution in Figure 2. The initial 2 mL of 0.3 mg/mL solution at pH 2 was undiluted (A), diluted to 4 mL (B), or diluted to 20 mL, with pH increasing from 2 to 3 (C). The initial absolute amounts of sulfuric acid and SOM available for browning reactions were the same in all cases, but the amount of time needed to fully evaporate the solution increased. The experiments showed that the effect was rather small. In doubling the volume of solvent (2 mL in Figure 2A vs 4 mL in Figure 2B), MAC values at 400 nm were approximately the same at 450 cm<sup>2</sup>/g. A 10-fold increase in volume of solvent (Figure 2C) resulted in a MAC at 400 nm of

610 cm<sup>2</sup>/g, representing an increase of 35%. This increase is visualized more easily in Figure 2D, comparing the evaporated MAC values from Figure 2A–C. Because browning takes place in the last stages of evaporation, it is perhaps not surprising that the extent of browning is not strongly dependent on the starting amount of water. On the basis of these findings, we expect variables other than solution volume, such as SOM type, to be more important for MAC values after evaporation.

For the largest volume of LIM/O<sub>3</sub> SOM (20 mL), the SOM was reconstituted in either 2 or 20 mL after the first evaporation (Figure 2C). The MAC values calculated from these two dilutions were the same, except in the vicinity of the 400 nm band. The change implies that the 400 nm band is likely due to acidic compounds and that the deprotonated forms of these compounds absorb more weakly than the neutral forms.

We also confirmed that the observed absorbance was proportional to the SOM concentration in solution (data not shown). The proportionality between absorbance and solution concentration suggests that the observed absorption for the evaporated extract arose from independent chromophores and was not due to intermolecular interactions between molecules, such as those found in charge-transfer complexes.<sup>19–21</sup>

The choice of evaporated solvent strongly affected the MAC values of the LIM/O<sub>3</sub> SOM, as shown in Figure 3. Three solvents commonly used to dissolve SOM were used here, namely, water (A), acetonitrile (B), and methanol (C). Updyke et al. (2012) showed that LIM/O<sub>3</sub> is fully extractable in water and methanol.<sup>22</sup> The similar MAC values observed in this work before the evaporation (Figure 3) suggest that all

three solvents fully extracted the LIM/O<sub>3</sub> SOM from the filter. In water, we see a distinctive peak at 400 nm after the evaporation, likely due to acidic forms of compounds being more absorbing, resulting in an enhancement in this region. Acetonitrile and methanol extracts have much higher MAC values after the evaporation, probably due to the fact that organic solvents are evaporated off more completely, making it possible to achieve higher acidity due to higher concentrations at the end of the evaporation process. Figure 3D compares MAC values after evaporation from Figure 3A–C on the same scale, clearly showing that the highest MAC values result from evaporation in methanol. Vapor pressures of methanol and acetonitrile are comparable; however, SOA carbonyl compounds in methanol are efficiently converted to hemiacetals, whereas they remain unchanged in acetonitrile.<sup>23,24</sup> The presence of hemiacetals in the starting mixture may contribute to the higher MAC values resulting from methanol evaporation.

**BrC Chromophores.** For the analysis of the possible products formed during the evaporative browning, we chose to focus on LIM/O<sub>3</sub> because its evaporation resulted in the largest increase in MAC values for all SOM types in this study (by a factor of 64 at 400 nm, Table 3). To avoid complications from hemiacetals present in methanol extract,<sup>23,24</sup> we only compared mass spectra in water and methanol. Figure 4 shows

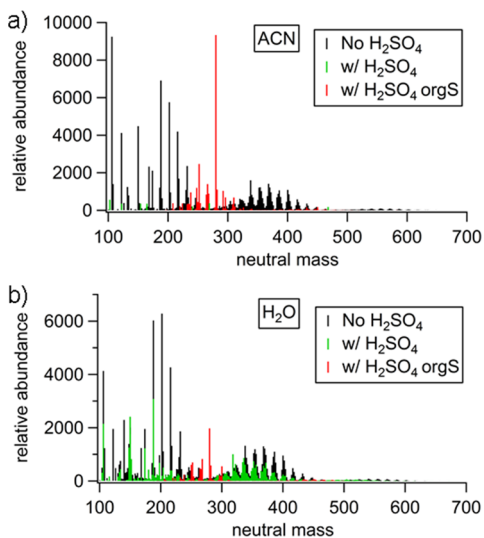


**Figure 4.** Combined positive and negative mass spectra when LIM/O<sub>3</sub> SOM is extracted in (a) acetonitrile and (b) water, then evaporated and redissolved in the extraction solvent. Peaks in green and red appear when sulfuric acid (H<sub>2</sub>SO<sub>4</sub>) is added prior to evaporation. Peaks in red contain sulfur and four or more oxygen atoms and are identified as potential organosulfates in this article. Peaks in black occur when sulfuric acid is not added. The largest red peak corresponds to C<sub>10</sub>H<sub>16</sub>SO<sub>7</sub>.

integrated ESI mass spectra for evaporated LIM/O<sub>3</sub> SOM extracted in acetonitrile (Figure 4a) or water (Figure 4b) in the presence or absence of sulfuric acid. Peaks corresponding to formulas with oxygen-to-sulfur ratios  $\geq 4$  are highlighted because they are potential organosulfate species. All possible organosulfate compounds were observed in the negative mode only; however, other masses were observed in both modes, and the abundances in mode were summed to give Figure 4. The acetonitrile extract has higher MACs by nearly a factor of 6 at 300 nm (Figure 3) compared with the water extract while

having a mass spectrum dominated by organosulfur compounds in the presence of sulfuric acid (Figure 4a). For the water extract evaporated in the presence of sulfuric acid, possible organosulfate species make up a lower fraction of total observed abundance. This implies that organosulfate compounds contribute to the pool of BrC species in the evaporated sample but does not rule out the possibility that other BrC compounds are simultaneously formed.

In both water and acetonitrile extracts, the most abundant organosulfate compound is C<sub>10</sub>H<sub>16</sub>SO<sub>7</sub> (Figure 4). This was also the most abundant organosulfate reported in previous experiments by Nguyen et al. (2012), who evaporated aqueous solutions of LIM/O<sub>3</sub> at pH values ranging from 2 to 9, and observed organosulfate formation at pH  $\leq 4$ .<sup>12</sup> The single ion chromatogram (SIC) for the corresponding ion with nominal *m/z* 279 in the negative mode is displayed in Figure 5. The SIC shows the presence of at least two major isomers of C<sub>10</sub>H<sub>16</sub>SO<sub>7</sub> in both extracts. Other prominent sulfur-containing compounds included C<sub>10</sub>H<sub>16</sub>SO<sub>5</sub>, C<sub>10</sub>H<sub>18</sub>SO<sub>6</sub>, C<sub>10</sub>H<sub>18</sub>SO<sub>7</sub>, and other compounds containing the original 10 carbon atoms from the limonene skeleton. There were many prominent C<sub>9</sub> compounds as well, likely formed from the oxidation of the exocyclic carbon–carbon double bond, producing molecules related to ketolimonalddehyde.<sup>25</sup> These compounds include C<sub>9</sub>H<sub>16</sub>SO<sub>6</sub>, C<sub>9</sub>H<sub>14</sub>SO<sub>8</sub>, C<sub>9</sub>H<sub>16</sub>SO<sub>7</sub>, and C<sub>9</sub>H<sub>14</sub>SO<sub>6</sub>.

The products observed during the evaporative browning may correlate to products of *D*-limonene ozonolysis formed in experiments with highly acidic seed particles. Inuma et al. prepared LIM/O<sub>3</sub> SOM in a chamber with sulfuric acid seed particles.<sup>26</sup> The SOM were extracted, evaporated to dryness, and reconstituted before the chemical analysis of organosulfates. The most prominent sulfur-containing ion they observed was C<sub>10</sub>H<sub>18</sub>SO<sub>7</sub>. The structure that they proposed, based off tandem ion fragmentation analysis, is shown in Figure 6a. The aldehyde and ketone functional groups result from ozone attacking the endocyclic double bond in *D*-limonene. An epoxide is then formed from ozone attacking the exocyclic double bond. Sulfuric acid attacks the epoxide, resulting in hydroxide and sulfate groups. We observed C<sub>10</sub>H<sub>18</sub>SO<sub>7</sub> in the water extract but not the acetonitrile extract.

The structure for C<sub>10</sub>H<sub>18</sub>SO<sub>7</sub> identified by Inuma et al.<sup>26</sup> provided evidence of the structures and formation mechanisms of related organosulfates. For example, the dehydration of C<sub>10</sub>H<sub>18</sub>SO<sub>7</sub> would give C<sub>10</sub>H<sub>16</sub>SO<sub>6</sub>, which is observed in the present study as the major product. Concentrated sulfuric acid is a classic desiccant, so it is conceivable that evaporating SOM in the presence of sulfuric acid dehydrates some of the SOM compounds. Dehydration results in the formation of carbon–carbon double bonds from alcohols, thus increasing the double bond equivalent (DBE) of the products. For example, in the absence of sulfuric acid, the abundance-weighted average DBE for all observed compounds is 4.4, whereas in the presence of sulfuric acid, it is 4.8. Additional evidence of the acid-catalyzed dehydration is shown in Figure 7. A number of the compounds formed in the presence of sulfuric acid are shifted to a lower *m/z*, compared with the nonacidified extract, by the exact molecular weight of water. Some of the compounds with high enough DBE may become sufficiently conjugated to absorb near-UV and visible radiation, accounting for the brown color of the residue formed in the evaporation.

We used HPLC-PDA-HRMS to determine specific elemental formulas for compounds that could contribute to

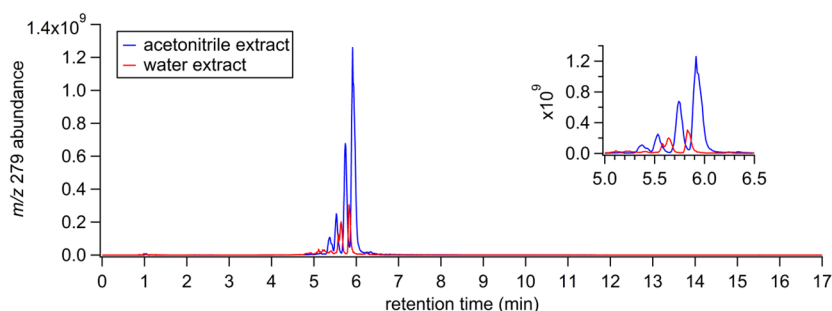


**Figure 5.** Single-ion chromatogram for the  $m/z$  279 ion in the negative mode, corresponding to  $C_{10}H_{16}SO_7$ . The acetonitrile extract is in blue, and the water extract is in red.

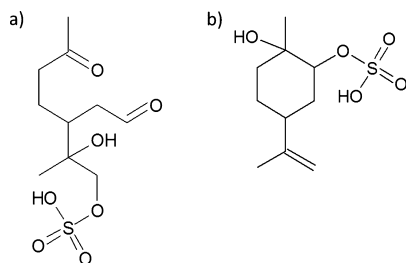


**Figure 6.** Structures of organosulfates: (a)  $C_{10}H_{18}SO_7$  reported in Iinuma et al. (2007)<sup>26</sup> based on  $MS^n$  analysis and (b)  $C_{10}H_{18}SO_5$  reported in Wang et al. (2017)<sup>31</sup> based on synthetic standards.

absorbance in the near-UV and visible ranges. Table 4 lists assigned chemical formulas for separated compounds that absorb in these ranges. They are listed by their chromatographic retention times, the absorption spectrum detected by the PDA, and the assigned chemical formula(s). Chromophores are also ranked by the abundance of each molecule in the individual mass spectrum in Figure 4, with 1 being the most abundant. All separated BrC chromophores are assigned as organosulfates and are observed in both acetonitrile and water extracts. Because of the limits in HPLC separation, we were not able to isolate and assign compounds responsible for the peak in absorption at 400 nm (Table 2); however, it is clear from the HPLC-PDA chromatogram in Figure 8 that there are multiple compounds absorbing into the visible region that elute between  $\sim 8$  and 12 min.

The first three chromophores in Table 4 have a  $C_{10}$  skeleton, suggesting that they are related to limonaldehyde in structure and, by extension, the structure in Figure 6a. However, they

have higher DBEs, presumably resulting from the acid-catalyzed dehydration discussed above. In addition, compounds containing 11 carbon atoms, such as  $C_{11}H_{16}SO_7$  and  $C_{11}H_{18}SO_8$ , were also observed. Such  $C_{11}$  compounds have been previously observed in the ozonolysis of monoterpenes,<sup>27–29</sup> but their formation mechanism is not clear. They presumably form by secondary reactions between the primary products, for example, reactions between  $C_{10}$  species and highly reactive formaldehyde,<sup>30</sup> which is a direct product of D-limonene ozonolysis.

## SUMMARY AND IMPLICATIONS

Ten types of SOM were solvent-extracted, evaporated in the presence of sulfuric acid, and redissolved to monitor and characterize the chemical changes occurring from a common physical process in the atmosphere for cloud, fog, and aqueous aerosol droplets. MAC values were measured during every step of the experiment, and, in general, the evaporation produced highly absorbing chromophores with absorption extending into the visible wavelength range. Most SOMs exhibited an increase in MAC after the evaporation, with the largest effect observed for LIM/ $O_3$ , LIM/OH, LIM/OH/ $NO_x$ , and ISO/OH/ $NO_x$ . Evaporating and redissolving SOM a second time did not result in a large change in MAC values. The MAC increase for LIM/ $O_3$  SOM was even higher when it was extracted in organic solvents (methanol and acetonitrile) and then evaporated, probably because more of the solvent could be evaporated by the rotary evaporator, resulting in a higher acidity of the residue. The structures of the proposed BrC chromophores are not known but could be similar to those shown in Figure 6. The mechanism by which the structure shown in Figure 6a is obtained was discussed by Iinuma et al.<sup>26</sup>

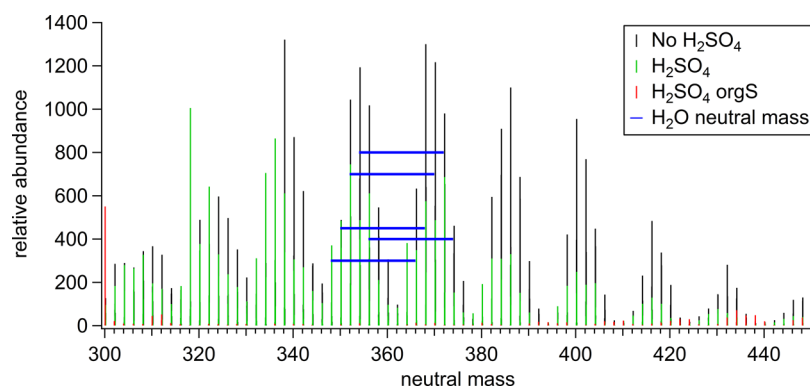


**Figure 7.** Dimer region of the mass spectrum corresponding to the LIM/ $O_3$  SOM water extract evaporated in the presence of sulfuric acid. Horizontal blue lines indicate the loss of water.

**Table 4.** Brown Carbon Chromophores in Evaporated ACN and H<sub>2</sub>O Extracts of LIM/O<sub>3</sub> SOM in the Presence of H<sub>2</sub>SO<sub>4</sub><sup>a</sup>

PDA retention time (min) (extract observed)	PDA spectrum	Assigned, neutral chemical formula	Ranking of abundance in mass spectrum (Fig 4)	
			ACN w/ H <sub>2</sub> SO <sub>4</sub>	H <sub>2</sub> O w/ H <sub>2</sub> SO <sub>4</sub>
5.90 (H <sub>2</sub> O), 5.78 (ACN)		C <sub>10</sub> H <sub>16</sub> SO <sub>6</sub> C <sub>10</sub> H <sub>18</sub> SO <sub>6</sub>	ACN w/ H <sub>2</sub> SO <sub>4</sub>	10
			H <sub>2</sub> O w/ H <sub>2</sub> SO <sub>4</sub>	30
6.05 (H <sub>2</sub> O)		C <sub>10</sub> H <sub>14</sub> SO <sub>6</sub>	ACN w/ H <sub>2</sub> SO <sub>4</sub>	7
			H <sub>2</sub> O w/ H <sub>2</sub> SO <sub>4</sub>	139
6.41 (ACN)		C <sub>10</sub> H <sub>16</sub> SO <sub>5</sub>	ACN w/ H <sub>2</sub> SO <sub>4</sub>	4
			H <sub>2</sub> O w/ H <sub>2</sub> SO <sub>4</sub>	482
6.50 (ACN)		C <sub>11</sub> H <sub>16</sub> SO <sub>7</sub>	ACN w/ H <sub>2</sub> SO <sub>4</sub>	7
			H <sub>2</sub> O w/ H <sub>2</sub> SO <sub>4</sub>	693
6.65 (ACN)		C <sub>11</sub> H <sub>18</sub> SO <sub>8</sub>	ACN w/ H <sub>2</sub> SO <sub>4</sub>	12
			H <sub>2</sub> O w/ H <sub>2</sub> SO <sub>4</sub>	276

<sup>a</sup>For each separated absorbance by HPLC, we give the observed PDA retention time, the PDA spectrum, the assigned neutral chemical formula, as well as the ranking of abundance in the mass spectrum of each extract, with the most abundant compound being first, or 1.

The structure in Figure 6b is formed from the acid-catalyzed ring opening of an epoxide by sulfuric acid and was observed in Wang et al.<sup>31</sup>

The abundance of organosulfates in ESI mass spectra may be related to higher MAC values in the visible region. The acetonitrile extract in the presence of sulfuric acid was dominated by organosulfates, whereas the water extract had a significant fraction of C<sub>x</sub>H<sub>y</sub>O<sub>z</sub> compounds. The organosulfates in this study had higher DBEs than those reported in Iinuma et al.<sup>26</sup> We postulate that sulfuric acid plays a role in acid-catalyzed dehydration reactions that result in more degrees of unsaturation. We separated five BrC chromophores, all of them organosulfates, including C<sub>10</sub>H<sub>16</sub>SO<sub>6</sub>, C<sub>10</sub>H<sub>14</sub>SO<sub>6</sub>, C<sub>10</sub>H<sub>16</sub>SO<sub>5</sub>, C<sub>11</sub>H<sub>16</sub>SO<sub>7</sub>, and C<sub>11</sub>H<sub>18</sub>SO<sub>8</sub>. This physical process of evaporation in the presence of sulfuric acid could cause a significant change in the optical properties of SOM under ambient conditions by making reactions produce more kinetically favorable organosulfates.

We should note that the VOC concentrations used for SOM preparation were relatively high in both the chamber (Table 1) and flow tube (Table 2) experiments, which tends to increase the weight of RO<sub>2</sub> + RO<sub>2</sub> reactions and the more efficient production of oligomeric compounds.<sup>32</sup> Furthermore, these experiments relied on SOM prepared under dry conditions. We were not in a position to carry out these experiments at lower VOC concentrations, and it is possible that the effects of evaporation will be different for more realistic SOM. The next logical step would be to test for the occurrence of these processes in field-collected SOM.

It is common when characterizing the organic fraction of particulate matter collected on filters to preconcentrate the extracts by solvent evaporation. Such a protocol enables organic analytes to be in the dynamic range of the detection method. Evaporation occurs in a fume hood under a stream of inert gas, such as nitrogen, or by a rotary evaporator. Light-absorbing organosulfate compounds could be potentially produced in this process as artifacts of acid-catalyzed reactions, such as those characterized in this study. In particular, externally mixed particle components could undergo chemical reactions in extracts if they did not originate in the same types

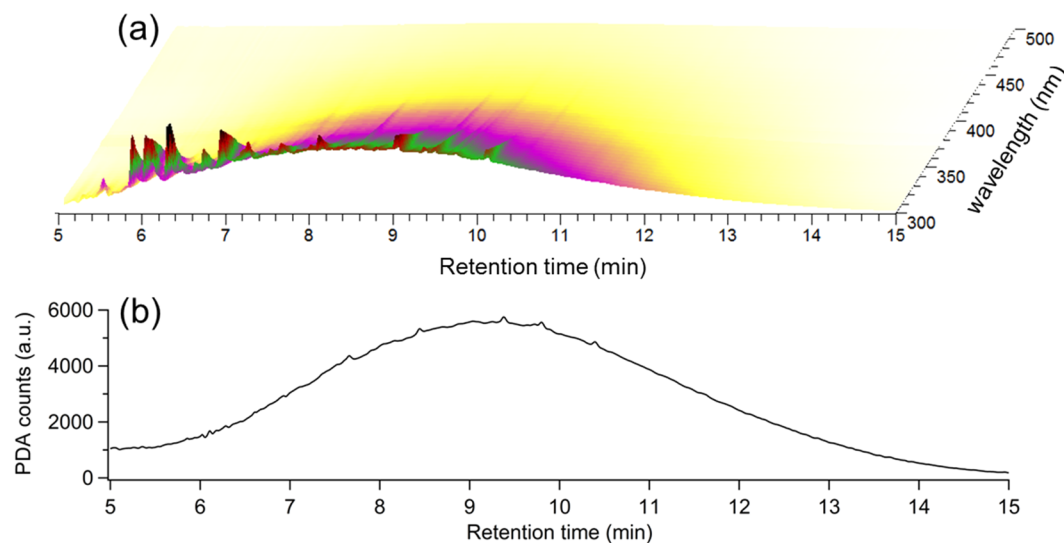


**Figure 8.** (a) 3D and (b) 2D HPLC-PDA chromatograms for the water LIM/O<sub>3</sub> SOM extract. Panel b shows the integrated PDA counts for 380 to 450 nm. Between 8 and 12 min, compounds absorbing visible light elute from the column and are largely unresolved.

of particles. The resulting evaporation reaction products could be mistakenly identified as species occurring in field or laboratory particles. The experiments described here approximate the conditions in the field and laboratory studies whereby producing these artifacts is feasible. For example, the concentration of particulate  $[H^+]$  measured in the Southeastern United States has been shown to reach  $10 \text{ nmol m}^{-3}$ .<sup>33</sup> Sampling such particles at 100 L/min for 1 day and extracting the filter in 1 mL of water would result in a pH of 3, which is close to the starting pH of 2 for the experiments described here. (We note that in the experiments by Nguyen et al. (2012), organosulfate formation was already observed for solutions evaporated from pH 4.) In the laboratory experiments, ammonium bisulfate seeds are commonly used in smog chambers to study acid-catalyzed reactions in particles. Injecting  $100 \mu\text{g m}^{-3}$  of ammonium bisulfate seeds, collecting  $1 \text{ m}^3$  of air from the chamber onto a filter, and then extracting the filter in 1 mL of water would also result in a pH of 3. Surratt et al. tested whether the organosulfates observed by LC/ESI-MS were due to sample preparation artifacts by spiking ISO/OH and APIN/OH/ $\text{NO}_x$  SOA with sulfuric acid.<sup>18</sup> They did not observe organosulfates in either extract. This paper reports no change in MAC values for ISO/OH (Table 3), in agreement with Surratt et al. However, this study did see an increase in MAC for APIN/OH/ $\text{NO}_x$  SOA following evaporation. We still recommend measuring the pH of aqueous extracts and ensuring that the pH is above 3 before evaporating to dryness. It is advised to avoid completely drying extracts (even organic extracts) and reconstituting them to prevent the spurious observation of organosulfates.

## AUTHOR INFORMATION

### Corresponding Author

\*E-mail: [nizkorod@uci.edu](mailto:nizkorod@uci.edu).

### ORCID

Lauren T. Fleming: [0000-0001-6495-6261](https://orcid.org/0000-0001-6495-6261)

Christian George: [0000-0003-1578-7056](https://orcid.org/0000-0003-1578-7056)

Sergey A. Nizkorodov: [0000-0003-0891-0052](https://orcid.org/0000-0003-0891-0052)

### Present Address

<sup>§</sup>S.L.B.: Department of Chemistry and Biochemistry, University of Colorado Boulder, UCB 215, Boulder, Colorado 80309, United States

### Author Contributions

The manuscript was written through contributions of all authors. All authors have given approval to the final version of the manuscript.

### Notes

The authors declare no competing financial interest.

## ACKNOWLEDGMENTS

S.A.N. thanks the Université Claude Bernard Lyon 1 for providing him with a visiting professorship in the summer of 2018. C.G. acknowledges support from the the Region Auvergne-Rhône-Alpes.

## REFERENCES

(1) Piccot, S. D.; Watson, J. J.; Jones, J. W. A Global Inventory of Volatile Organic Compound Emissions from Anthropogenic Sources. *J. Geophys. Res. Atmos.* **1992**, *97* (D9), 9897–9912.

(2) Lamb, B.; Westberg, H.; Allwine, G.; Quarles, T. Biogenic Hydrocarbon Emissions from Deciduous and Coniferous Trees in the United States. *J. Geophys. Res.* **1985**, *90* (D1), 2380.

(3) World Health Organization, W. H. Indoor Air Quality: Organic Pollutants. *Environ. Technol. Lett.* **1989**, *10* (9), 855–858.

(4) Boucher, O.; Anderson, T. L. General Circulation Model Assessment of the Sensitivity of Direct Climate Forcing by Anthropogenic Sulfate Aerosols to Aerosol Size and Chemistry. *J. Geophys. Res.* **1995**, *100* (D12), 26117.

(5) IPCC. *Climate Change 2013: The Physical Science Basis. Contribution of Working Group I to the Fifth Assessment Report of the Intergovernmental Panel on Climate Change*; Stocker, T. F., Qin, D., Plattner, G.-K., Tignor, M., Allen, S. K., Boschung, J., Nauels, A., Xia, Y., Bex, V., Midgley, P. M., Eds.; Cambridge University Press: Cambridge, U.K., 2013.

(6) Finlayson-Pitts, B. J.; Pitts, J. N. *Chemistry of the Upper and Lower Atmosphere: Theory, Experiments, and Applications*; Academic Press: San Diego, CA, 2000.

(7) Minerath, E. C.; Casale, M. T.; Elrod, M. J. Kinetics Feasibility Study of Alcohol Sulfate Esterification Reactions in Tropospheric Aerosols. *Environ. Sci. Technol.* **2008**, *42* (12), 4410–4415.

(8) Minerath, E. C.; Elrod, M. J. Assessing the Potential for Diol and Hydroxy Sulfate Ester Formation from the Reaction of Epoxides in Tropospheric Aerosols. *Environ. Sci. Technol.* **2009**, *43* (5), 1386–1392.

(9) Darer, A. I.; Cole-Filipiak, N. C.; O'Connor, A. E.; Elrod, M. J. Formation and Stability of Atmospherically Relevant Isoprene-Derived Organosulfates and Organonitrates. *Environ. Sci. Technol.* **2011**, *45* (5), 1895–1902.

(10) Eddingsaas, N. C.; VanderVelde, D. G.; Wennberg, P. O. Kinetics and Products of the Acid-Catalyzed Ring-Opening of Atmospherically Relevant Butyl Epoxy Alcohols. *J. Phys. Chem. A* **2010**, *114* (31), 8106–8113.

(11) Budisulistiorini, S. H.; Li, X.; Bairai, S. T.; Renfro, J.; Liu, Y.; Liu, Y. J.; McKinney, K. A.; Martin, S. T.; McNeill, V. F.; Pye, H. O. T.; et al. Examining the Effects of Anthropogenic Emissions on Isoprene-Derived Secondary Organic Aerosol Formation during the 2013 Southern Oxidant and Aerosol Study (SOAS) at the Look Rock, Tennessee Ground Site. *Atmos. Chem. Phys.* **2015**, *15* (15), 8871–8888.

(12) Nguyen, T. B.; Lee, P. B.; Updyke, K. M.; Bones, D. L.; Laskin, J.; Laskin, A.; Nizkorodov, S. A. Formation of Nitrogen- and Sulfur-Containing Light-Absorbing Compounds Accelerated by Evaporation of Water from Secondary Organic Aerosols. *J. Geophys. Res.: Atmos.* **2012**, *117* (D1), D01207.

(13) Hallquist, M.; Wenger, J. C.; Baltensperger, U.; Rudich, Y.; Simpson, D.; Claeys, M.; Dommen, J.; Donahue, N. M.; George, C.; Goldstein, A. H.; et al. The Formation, Properties and Impact of Secondary Organic Aerosol: Current and Emerging Issues. *Atmos. Chem. Phys.* **2009**, *9* (14), 5155–5236.

(14) Bones, D. L.; Henricksen, D. K.; Mang, S. A.; Gonsior, M.; Bateman, A. P.; Nguyen, T. B.; Cooper, W. J.; Nizkorodov, S. A. Appearance of Strong Absorbers and Fluorophores in Limonene- $\text{O}_3$  Secondary Organic Aerosol Due to  $\text{NH}_4^+$ -Mediated Chemical Aging over Long Time Scales. *J. Geophys. Res.* **2010**, *115* (D5), D05203.

(15) Romonosky, D. E.; Ali, N. N.; Saiduddin, M. N.; Wu, M.; Lee, H. J.; Aiona, P. K.; Nizkorodov, S. A. Effective Absorption Cross Sections and Photolysis Rates of Anthropogenic and Biogenic Secondary Organic Aerosols. *Atmos. Environ.* **2016**, *130*, 172–179.

(16) Pluskal, T.; Castillo, S.; Villar-Briones, A.; Orešič, M. MZmine 2: Modular Framework for Processing, Visualizing, and Analyzing Mass Spectrometry-Based Molecular Profile Data. *BMC Bioinf.* **2010**, *11* (1), 395.

(17) Surratt, J. D.; Gómez-González, Y.; Chan, A. W. H.; Vermeylen, R.; Shahgholi, M.; Kleindienst, T. E.; Edney, E. O.; Offenberg, J. H.; Lewandowski, M.; Jaoui, M.; et al. Organosulfate Formation in Biogenic Secondary Organic Aerosol. *J. Phys. Chem. A* **2008**, *112* (36), 8345–8378.

(18) Surratt, J. D.; Kroll, J. H.; Kleindienst, T. E.; Edney, E. O.; Claeys, M.; Sorooshian, A.; Ng, N. L.; Offenberg, J. H.; Lewandowski, M.; Jaoui, M.; et al. Evidence for Organosulfates in Secondary Organic Aerosol. *Environ. Sci. Technol.* **2007**, *41* (2), 517–527.

(19) Phillips, S. M.; Smith, G. D. Light Absorption by Charge Transfer Complexes in Brown Carbon Aerosols. *Environ. Sci. Technol. Lett.* **2014**, *1* (10), 382–386.

(20) Phillips, S. M.; Smith, G. D. Further Evidence for Charge Transfer Complexes in Brown Carbon Aerosols from Excitation–Emission Matrix Fluorescence Spectroscopy. *J. Phys. Chem. A* **2015**, *119* (19), 4545–4551.

(21) Sharpless, C. M.; Blough, N. V. The Importance of Charge-Transfer Interactions in Determining Chromophoric Dissolved Organic Matter (CDOM) Optical and Photochemical Properties. *Environ. Sci. Process. Impacts* **2014**, *16* (4), 654–671.

(22) Updyke, K. M.; Nguyen, T. B.; Nizkorodov, S. A. Formation of Brown Carbon via Reactions of Ammonia with Secondary Organic Aerosols from Biogenic and Anthropogenic Precursors. *Atmos. Environ.* **2012**, *63*, 22–31.

(23) Bateman, A. P.; Walser, M. L.; Desyaterik, Y.; Laskin, J.; Laskin, A.; Nizkorodov, S. A. The Effect of Solvent on the Analysis of Secondary Organic Aerosol Using Electrospray Ionization Mass Spectrometry. *Environ. Sci. Technol.* **2008**, *42* (19), 7341–7346.

(24) Romonosky, D. E.; Laskin, A.; Laskin, J.; Nizkorodov, S. A. High-Resolution Mass Spectrometry and Molecular Characterization of Aqueous Photochemistry Products of Common Types of Secondary Organic Aerosols. *J. Phys. Chem. A* **2015**, *119* (11), 2594–2606.

(25) Nguyen, T. B.; Laskin, A.; Laskin, J.; Nizkorodov, S. A. Brown Carbon Formation from Ketoaldehydes of Biogenic Monoterpenes. *Faraday Discuss.* **2013**, *165* (0), 473.

(26) Iinuma, Y.; Müller, C.; Böge, O.; Gnauk, T.; Herrmann, H. The Formation of Organic Sulfate Esters in the Limonene Ozonolysis Secondary Organic Aerosol (SOA) under Acidic Conditions. *Atmos. Environ.* **2007**, *41* (27), 5571–5583.

(27) Bateman, A. P.; Nizkorodov, S. A.; Laskin, J.; Laskin, A. Time-Resolved Molecular Characterization of Limonene/Ozone Aerosol Using High-Resolution Electrospray Ionization Mass Spectrometry. *Phys. Chem. Chem. Phys.* **2009**, *11* (36), 7931.

(28) Walser, M. L.; Desyaterik, Y.; Laskin, J.; Laskin, A.; Nizkorodov, S. A. High-Resolution Mass Spectrometric Analysis of Secondary Organic Aerosol Produced by Ozonation of Limonene. *Phys. Chem. Chem. Phys.* **2008**, *10* (7), 1009–1022.

(29) Tu, P.; Hall, W. A.; Johnston, M. V. Characterization of Highly Oxidized Molecules in Fresh and Aged Biogenic Secondary Organic Aerosol. *Anal. Chem.* **2016**, *88* (8), 4495–4501.

(30) Nguyen, T. B.; Bateman, A. P.; Bones, D. L.; Nizkorodov, S. A.; Laskin, J.; Laskin, A. High-Resolution Mass Spectrometry Analysis of Secondary Organic Aerosol Generated by Ozonolysis of Isoprene. *Atmos. Environ.* **2010**, *44* (8), 1032–1042.

(31) Wang, Y.; Hu, M.; Lin, P.; Guo, Q.; Wu, Z.; Li, M.; Zeng, L.; Song, Y.; Zeng, L.; Wu, Y.; et al. Molecular Characterization of Nitrogen-Containing Organic Compounds in Humic-like Substances Emitted from Straw Residue Burning. *Environ. Sci. Technol.* **2017**, *51* (11), 5951–5961.

(32) Kourtchev, I.; Giorio, C.; Manninen, A.; Wilson, E.; Mahon, B.; Aalto, J.; Kajos, M.; Venables, D.; Ruuskanen, T.; Levula, J.; et al. Enhanced Volatile Organic Compounds Emissions and Organic Aerosol Mass Increase the Oligomer Content of Atmospheric Aerosols. *Sci. Rep.* **2016**, *6* (1), 35038.

(33) Guo, H.; Xu, L.; Bougiatioti, A.; Cerully, K. M.; Capps, S. L.; Hite, J. R.; Carlton, A. G.; Lee, S.-H.; Bergin, M. H.; Ng, N. L.; et al. Fine-Particle Water and PH in the Southeastern United States. *Atmos. Chem. Phys.* **2015**, *15* (9), 5211–5228.